SEARCH FOR DARK MATTER IN MONO-JET AND MONO-PHOTON EVENTS AT ATLAS

Philippe Calfayan
(Ludwig-Maximilians Universität, München)

July 16, 2012

Dark Matter candidates and detection

- We assume there is an interaction between SM and dark sector, not necessarily the weak one. In the following, we equally refer to "WIMP" or "Dark Matter" (DM) particle to describe a DM candidate.

- DM candidate must fulfill the following requirements:
  - Massive
  - Neutral
  - Interact weakly with Standard Model (SM) particles
  - Stable (detector time scale)

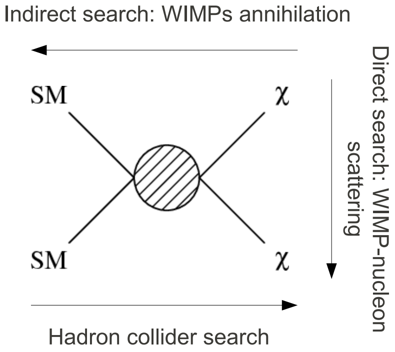

Search for Dark Matter at Hadron Collider

- Case where new SM/DM mediators heavier than DM can be produced directly

  e.g.: cascade decays of supersymmetric (SUSY) particles down to a stable neutralino (LSP)

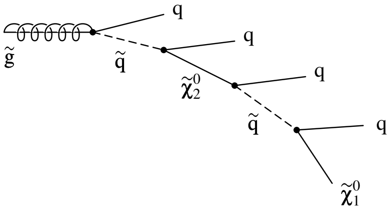

- Case where all new particles mediating the interaction between DM candidate and SM particles are too heavy to be produced directly at LHC

⇒ DM production via contact interactions [Maverick Dark Matter, hep-ph/1002.4137]

SM/DM coupling proportional to a suppression scale $M_\star$

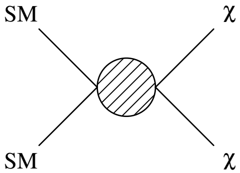

Assumptions on DM candidate pair production via contact interaction

- All new particles mediating the interaction between DM candidate and SM particles are too heavy to be produced directly
- Interaction between DM and SM not explicitly via weak interactions
- DM particles are assumed to be Dirac fermions (Majorana fermions would lead to higher production cross section)
- Out of 14 operators for Dirac fermions, 4 categories are distinguished according to $\not{E}_T$ shapes: D1, D5, D9, D11 (D8 in same category as D5)
- DM particle couple to SM light quarks or gluons universally and with one given operator exclusively

Name	Initial state	Type	Operator
D1	qq	scalar	$\frac{m_q}{M_\star^3}\bar{\chi}\chi\bar{q}q$
D5	qq	vector	$\frac{1}{M_\star^2}\bar{\chi}\gamma^\mu\chi\bar{q}\gamma_\mu q$
D8	qq	axial-vector	$\frac{1}{M_\star^2}\bar{\chi}\gamma^\mu\gamma^5\chi\bar{q}\gamma_\mu\gamma^5 q$
D9	qq	tensor	$\frac{1}{M_\star^2}\bar{\chi}\sigma^{\mu\nu}\chi\bar{q}\sigma_{\mu\nu}q$
D11	gg	scalar	$\frac{1}{4M_\star^3}\bar{\chi}\chi\alpha_s(G^a_{\mu\nu})^2$

- The effective theory must be valid for given the parameters $M_\star$ and m_χ (DM particle mass)

Search for Dark Matter at ATLAS

- DM particle pairs are very weakly interacting with SM particles and evade the detector, which results in missing transverse energy ($\not{E}_T$)
- To tag events with pair-produced DM particles, a jet or a photon from initial state radiation (ISR) is required

⇒ **Two signatures are investigated: mono-jet+$\not{E}_T$ and mono-photon+$\not{E}_T$**

Analyses are based on the complete 2011 ATLAS *pp* dataset ($4.7\,\mathrm{fb}^{-1}$)

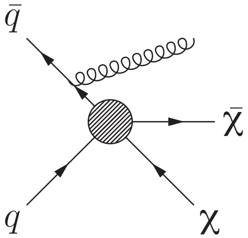

Event selections

Mono-jet analysis:

- $\not{E}_T$ trigger (98% efficient at $120\,\mathrm{GeV}$)
- primary vertex with ≥ 2 tracks
- central leading jet ($|\eta| < 2$)
- $|\Delta\Phi(jet_2, \not{E}_T)| > 0.5$
- no more than 2 jets with $p_T > 30\,\mathrm{GeV}$ and $|\eta| < 4.5$
- no e with $p_T > 20\,\mathrm{GeV}$ and $|\eta| < 2.47$
- no μ with $p_T > 7\,\mathrm{GeV}$ and $|\eta| < 2.5$
- Signal regions (SR) with symmetric lower cut on leading jet p_T and $\not{E}_T$: $120, 220, 350, 500\,\mathrm{GeV}$

Mono-photon analysis:

- $\not{E}_T$ trigger (98% efficient at $150\,\mathrm{GeV}$)
- primary vertex with ≥ 5 tracks
- leading photon fulfills: $p_T > 150\,\mathrm{GeV}$, $|\eta| < 2.37$ excluding calorimeter barrel/endcap transition region ($1.37 < |\eta| < 1.52$)
- overlap removal:
  $|\Delta\Phi(\gamma, \not{E}_T)| > 0.4$
  $|\Delta R(jet, \gamma)| > 0.4$
  $|\Delta\Phi(jet, \not{E}_T)| > 0.4$
- no more than 1 jet with $p_T > 30\,\mathrm{GeV}$ and $|\eta| < 4.5$
- no e with $p_T > 20\,\mathrm{GeV}$ and $|\eta| < 2.47$
- no μ with $p_T > 10\,\mathrm{GeV}$ and $|\eta| < 2.5$

Backgrounds from the Standard Model

Mono-jet analysis:

- Electroweak processes (determined using data control regions)
  - $Z(\to \nu\nu)$+jets
  - $W(\to \ell\nu)$+jets
  - $Z(\to \ell\ell)$+jets
- Top quark production (from simulation)
- Multi-jet production (from Data)
- Non-collision background (from Data)
- *WW*, *WZ*, *ZZ* di-boson production (from simulation)
- $\gamma + \text{jets}$ (negligible)

Mono-photon analysis:

- Electroweak processes (determined using data control regions)
  - $Z \to \nu\nu + \gamma$
  - $W \to \ell\nu + \gamma$
  - $Z \to \ell\ell + \gamma$
  - W/Z+jets
- $\gamma +$ *jet* and multi-jet production (from Data)
- Top quark production (from simulation)
- $\gamma\gamma$ processes (from simulation)
- Di-boson production (from simulation)
- Non-collision background (negligible)

Data-driven EW background determination [mono-jet analysis]

- For each SR, EW background is determined using **4 control regions (CR)** similar to EW processes in SR but with leptonic W/Z decays:

SR	$Z \to \nu\bar{\nu}$+jets	$W \to \tau\nu$+jets $W \to \mu\nu$+jets	$W \to e\nu$+jets	$Z \to \tau^+\tau^-$+jets $Z \to \mu^+\mu^-$+jets
CR	$W \to e\nu$+jets $W \to \mu\nu$+jets $Z \to e^+e^-$+jets $Z \to \mu^+\mu^-$+jets	$W \to \mu\nu$+jets	$W \to e\nu$+jets	$Z \to \mu^+\mu^-$+jets

- Jets modeling and pile-up are taken from data:

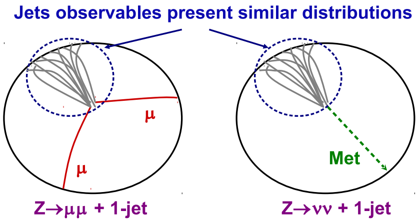

- **4 CR per SR to determine $Z(\to \nu\nu)$+jets $\to$ 4 measurements are combined**

Data-driven EW background determination [mono-jet analysis]

- Each EW background process is determined with the following steps:
  1. Select Data events in CR
  2. Remove the background to the CR.
     Multi-jet background estimated from Data is subtracted directly, while other background processes (EW,top,di-bosons) are accounted for by estimating the simulated fraction of the EW process to determine.
  3. Correct for the CR-specific cuts (lepton acceptance, M($\ell\ell$) or M(ℓ, $\not{E}_T$), trigger selection) to get to the full lepton phase space
  4. Transfer from the full lepton phase space to SR (accounts for phase space, cross section and Br differences)

$$N_{SR}^{predicted} = (N_{CR}^{Data} - N_{Multi-jet}^{Data}) \times F_{EW}^{MC} \times C_{CR} \times \frac{N_{SR}^{MC}}{N_{jet\,/\,\not{E}_T}^{MC}}$$

→ Corrections to the data CR only rely on ratios of simulated samples

→ Shapes of variables involved in CR-specific cuts are required to be well modeled by simulation to validate C_{CR}

→ All corrections are applied bin-by-bin, as function of SR variable to determine

Muon control region

- Except the lepton and W/Z selection, all control regions (for signal regions 1, 2, 3 and 4) use the the same cuts as in the signal region

- $Z(\to \mu\mu)$+jets:
  - $\not{E}_T$ trigger
  - exactly 2 muons
  - $66 < \frac{M_{\mu\mu}}{\mathrm{GeV}} < 116$

- $W(\to \mu\nu)$+jets:
  - $\not{E}_T$ trigger
  - exactly 1 muon
  - $\not{E}_T(calo - muon) > 25\,\mathrm{GeV}$
  - $M_T(\mu, \not{E}_T) > 40\,\mathrm{GeV}$

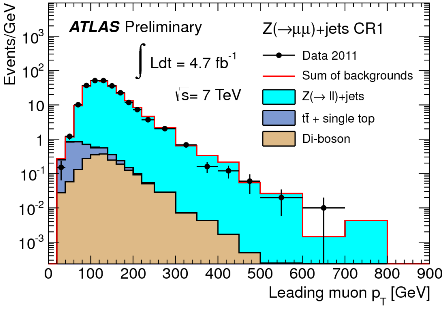

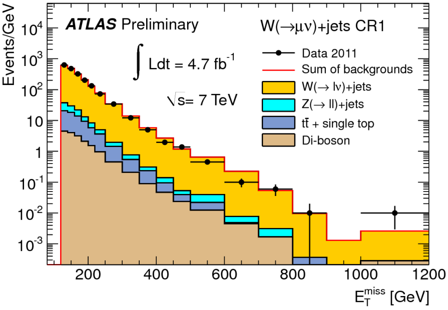

Electron control region

- Except the lepton and W/Z selection, all control regions (for signal regions 1, 2, 3 and 4) use the the same cuts as in the signal region

- $Z(\rightarrow ee)$+jets:
  - electron trigger
  - exactly 2 electrons
  - $66 < \frac{M_{ee}}{\text{GeV}} < 116$

- $W(\rightarrow e\nu)$+jets:
  - $\not{E}_T$ trigger
  - exactly 1 electron
  - $\not{E}_T(calo + electron) > 25\,\text{GeV}$
  - $40 < \frac{M_T(e, \not{E}_T)}{\text{GeV}} < 100$

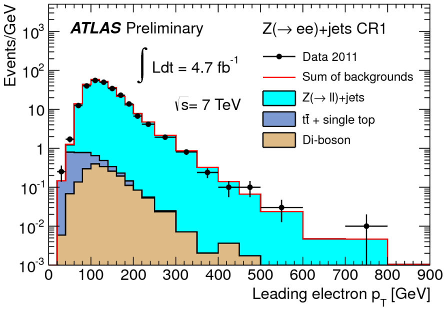

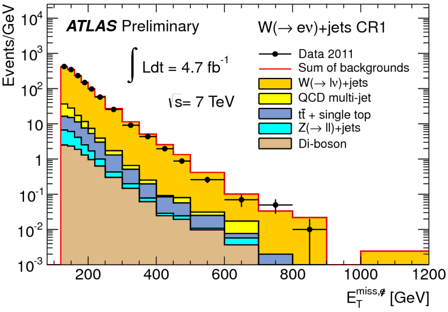

Mono-jet analysis results

Signal region 1:

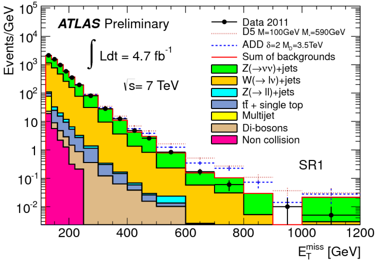

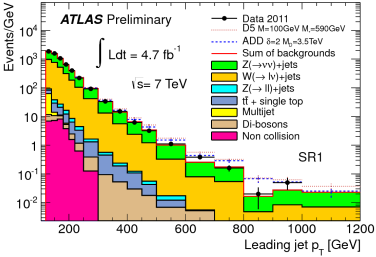

Signal region 4:

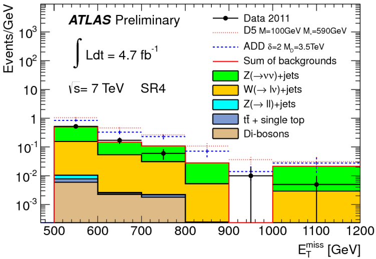

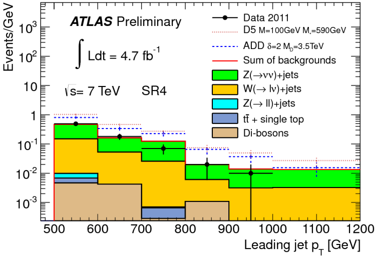

Mono-jet analysis results

	SR1	SR2	SR3	SR4
$Z \to \nu\bar{\nu}$+jets	63000 ± 2100	5300 ± 280	500 ± 40	58 ± 9
$W \to \tau\nu$+jets	31400 ± 1000	1853 ± 81	133 ± 13	13 ± 3
$W \to e\nu$+jets	14600 ± 500	679 ± 43	40 ± 8	5 ± 2
$W \to \mu\nu$+jets	11100 ± 600	704 ± 60	55 ± 6	6 ± 1
$t\bar{t}$ + single t	1240 ± 250	57 ± 12	4 ± 1	-
Multijets	1100 ± 900	64 ± 64	8^{+9}_{-8}	-
Non-coll. Background	575 ± 83	25 ± 13	-	-
$Z/\gamma^* \to \tau\tau$+jets	421 ± 25	15 ± 2	2 ± 1	-
Di-bosons	302 ± 61	29 ± 5	5 ± 1	1 ± 1
$Z/\gamma^* \to \mu\mu$+jets	204 ± 19	8 ± 4	-	-
Total Background	124000 ± 4000	8800 ± 400	750 ± 60	83 ± 14
Events in Data (4.7 fb^{-1})	124703	8631	785	77
$\sigma_{\text{vis}}^{\text{obs}}$ at 90% [pb]	1.63	0.13	0.026	0.006
$\sigma_{\text{vis}}^{\text{exp}}$ at 90% [pb]	1.54	0.15	0.020	0.006
$\sigma_{\text{vis}}^{\text{obs}}$ at 95% [pb]	1.92	0.16	0.030	0.007
$\sigma_{\text{vis}}^{\text{exp}}$ at 95% [pb]	1.82	0.17	0.024	0.008

- The observed data is consistent with the prediction from the SM

→ 90% and 95% confidence level (CL) upper bounds on the visible cross section ($\sigma \times A \times \epsilon$) are set (values of A and ϵ provided in public results)

Mono-photon analysis results

Background source	Prediction	± (stat.)	± (syst.)
$Z(\to \nu\bar{\nu}) + \gamma$	93	± 16	± 8
$Z/\gamma^{*}(\to \ell^{+}\ell^{-}) + \gamma$	0.4	± 0.2	± 0.1
$W(\to \ell\nu) + \gamma$	24	± 5	± 2
W/Z + jets	18	–	± 6
top	0.07	± 0.07	± 0.01
$WW, WZ, ZZ, \gamma\gamma$	0.3	± 0.1	± 0.1
γ+jets and multi-jet	1.0	–	± 0.5
Non-collision background	–	–	–
Total background	137	± 18	± 9
Events in data (4.6 fb^{-1})	116		

- The observed data is consistent with the prediction from the SM

→ Upper limits on the visible cross section ($\sigma \times A \times \epsilon$) are computed:

- ○ 90% CL: 5.6 fb
- ○ 95% CL: 6.8 fb

(values of A and ϵ provided in public results)

Signal region:

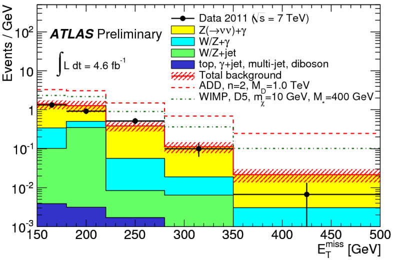

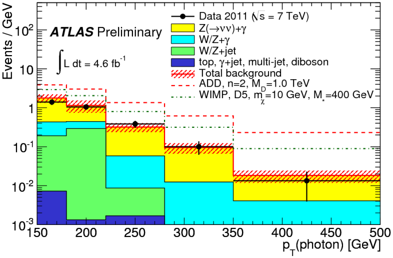

Limits on the suppresion scale $M_\star$ [mono-jet analysis]

- Lower limits at 90% CL on $M_\star$ are computed as function of the DM particle mass m_χ, for different DM/SM couplings
- SR3 is used for operators D1 and D5, while SR4 is utilized for D9 and D11 (based on sensitivity)

Name	Initial state	Type	Operator
D1	qq	scalar	$\frac{m_q}{M_\star^3}\bar{\chi}\chi\bar{q}q$
D5	qq	vector	$\frac{1}{M_\star^2}\bar{\chi}\gamma^\mu\chi\bar{q}\gamma_\mu q$
D8	qq	axial-vector	$\frac{1}{M_\star^2}\bar{\chi}\gamma^\mu\gamma^5\chi\bar{q}\gamma_\mu\gamma^5 q$
D9	qq	tensor	$\frac{1}{M_\star^2}\bar{\chi}\sigma^{\mu\nu}\chi\bar{q}\sigma_{\mu\nu}q$
D11	gg	scalar	$\frac{1}{4M_\star^3}\bar{\chi}\chi\alpha_s(G^a_{\mu\nu})^2$

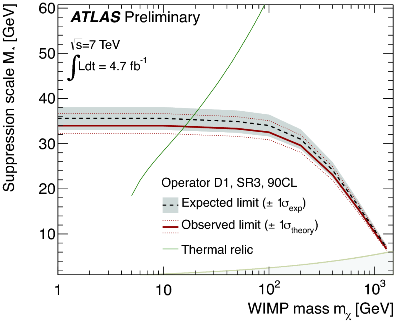

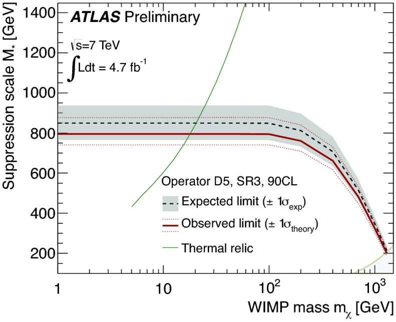

Limits on the suppresion scale $M_\star$ [mono-jet analysis]

$$\boxed{\Omega_\chi \propto \frac{1}{<\sigma\nu>} \sim \frac{m_\chi^2}{g_\chi^4}} \text{ with } \begin{cases} \Omega_\chi: & \text{observed thermal relic density} \sim 0.24 \\ \langle\sigma\nu\rangle: & \text{thermally-averaged annihilation cross section} \\ m_\chi: & \text{DM particle mass} \\ g_\chi: & \text{coupling between DM and SM particles} \end{cases}$$

- Thermal relic density observed by WMAP (green curve) is compatible with DM having couplings and mass comparable to weak scale masses and weak force

→ If $M_\star$ above relic line, other annihilation processes are required to stay consistent with WMAP results (here: annihilation to light q via 1 given operator exclusively)

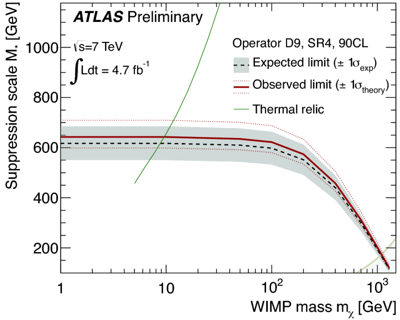

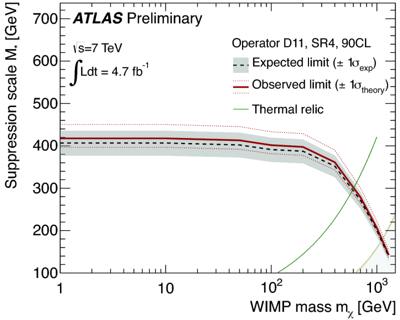

Limits on WIMP-nucleon scattering cross section [mono-jet analysis]

- Bounds on $M_\star$ can be converted to bounds on WIMP-nucleon scattering in the effective operator approach

$\rightarrow$ Comparison with direct DM detection experiments:

- **Spin-independent interaction:**

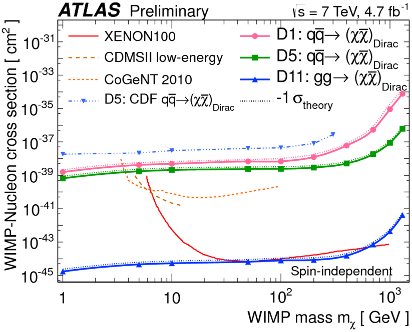

$\Rightarrow$ ATLAS more sensitive for D1 & D5 at low m_χ region, and for D11 at $\sim$ any m_χ

- **Spin-dependent interaction:**

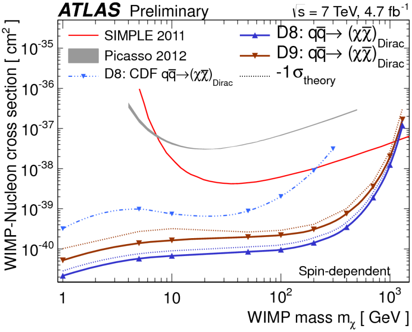

$\Rightarrow$ ATLAS limits stronger for D8 & D9

Limits on WIMP-nucleon scattering cross section [mono-photon analysis]

- Bounds on $M_\star$ can be converted to bounds on WIMP-nucleon scattering in the effective operator approach

→ Comparison with direct DM detection experiments:

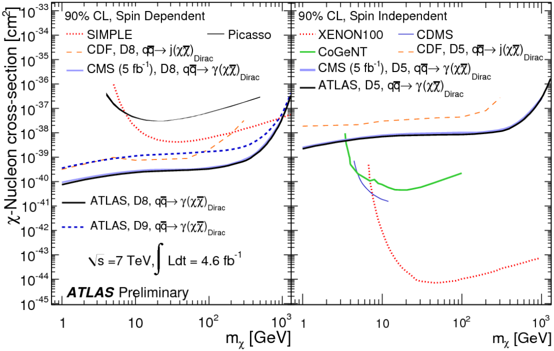

(same conclusion as with the mono-jet analysis)

Limits on Dark Matter annihilation cross section

- Bounds on vector and axial-vector interactions can be translated into cross section upper limits on WIMP annihilations to 4 light q (flavor universal interaction)
- The results are compared to the annihilations to bb from Galactic high energy gamma ray observations by Fermi LAT

- Results are comparable and complementary
- Below 10 GeV for D5 and 70 GeV for D8, ATLAS limits below relic value
  $\rightarrow$ abundance not consistent with WMAP
- Annihilation of Majorana fermions is 2$\times$ larger than that of Dirac fermions

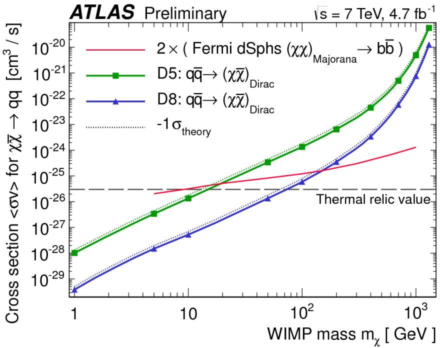

Summary

- Searches for physics beyond Standard Model in events with mono-jet and mono-photon signatures are performed with the full 2011 pp dataset

  http://atlas.web.cern.ch/Atlas/GROUPS/PHYSICS/CONFNOTES/ATLAS-CONF-2012-085/

  http://atlas.web.cern.ch/Atlas/GROUPS/PHYSICS/CONFNOTES/ATLAS-CONF-2012-084/

- Data-driven techniques allowed to understand background from SM with very good precision
- Observed data agrees with the expectation from the SM within uncertainties
- Contact interactions are considered in order to model the DM/SM couplings
  $\Rightarrow$ two parameters: suppression scale and DM particle mass
- ATLAS lower bounds on the suppression scale are converted into limits on WIMP-nucleon scattering and WIMP annihilation cross sections
- ATLAS results are compared to DM searches from Astroparticle experiments, and prove to be complementary

BACKUP

Mono-photon event candidate

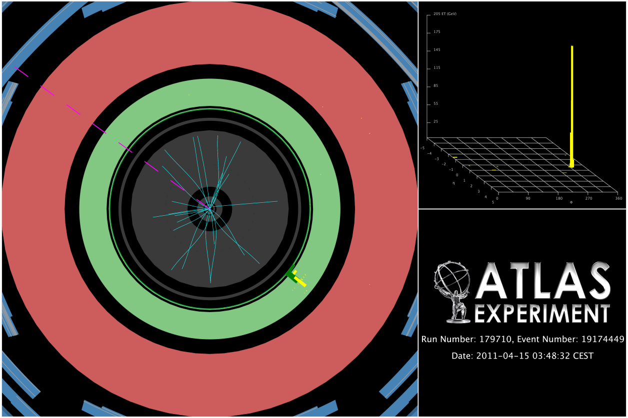

$\not{E}_T = 218.3\,\mathrm{GeV}$
$\Phi(\not{E}_T) = 2.52$
$p_T^{\gamma} = 218.0\,\mathrm{GeV}$
$\eta^{\gamma} = 0.39$
$\phi^{\gamma} = -0.68$
No jets in the final state

Data-driven determination of the non-collision background

- Beam background muons can deposit significant energy (up to ~TeV) in the colorimeters that can be reconstructed as fake jets.

- Fake jets are balanced by MET.
  - Therefore, they lead to similar event topology as monojet signals.
  - They fire MET triggers.

➡ Monojet analysis requires efficient fake jet removal.

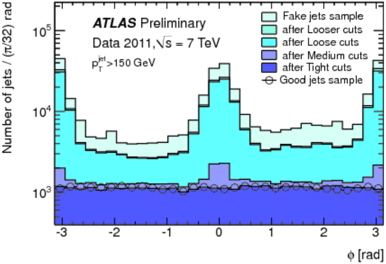

- Jet cleaning techniques based on jet quality criteria (e.g. jet charged fraction, electromagnetic fraction) provide efficient rejection at the level of 10^{-3}.

- Residual level of non-collision backgrounds is estimated with dedicated tool that searches for signatures of particles traversing the detector parallel to the beam pipe.

Systematic uncertainties in the mono-jet analysis

Source	SR1	SR2	SR3	SR4
JES/JER/$E_{\mathrm{T}}^{\mathrm{miss}}$	1.0	2.6	4.9	5.8
MC Z/W modelling	2.9	2.9	2.9	3.0
MC stat. uncert.	0.5	1.4	3.4	8.9
$1 - f_{\mathrm{EW}}$	1.0	1.0	0.7	0.7
Muon scale and resolution	0.03	0.02	0.08	0.61
Lepton scale factors	0.4	0.5	0.6	0.7
Multijet BG in electron CR	0.1	0.1	0.3	0.6
Di-boson, top, multijet, non-collisions	0.8	0.7	1.1	0.3
Total systematic uncertainty	3.4	4.4	6.8	11.1
Total statistical uncertainty	0.5	1.7	4.3	11.8

Interpretation in terms of ADD LED model (1)

- Models of large extra dimensions can provide an essential ingredient to a solution to the hierarchy problem.
- Arkani-Hamed, Dimopoulos, Dvali (ADD) model
  - Gravity propagates in (4+n)-dimensional bulk space.
  - Standard Model fields are confined to 4 dimensions.

$$M_{Pl}{}^2 \sim M_D{}^{2+n} R^n$$

M_{Pl} = 4-dimensional Planck scale
M_D = fundamental (4+n)-dimensional Planck scale
n = number of the extra dimensions
R = size of the extra dimensions

  - The extra spatial dimensions are compactified resulting in Kaluza-Klein towers of massive graviton modes.
  - At LHC, gravitons can be produced in association with jets or photons, leading to monojet or monophoton detector signatures.

$$\begin{aligned} qg &\to qG \\ gg &\to gG \\ q\bar{q} &\to gG, \gamma G \end{aligned}$$

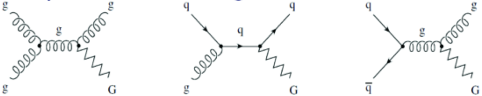

Interpretation in terms of ADD LED model (2)

- Theoretical uncertainties on ADD are associated with PDF uncertainties, ISR/FSR, factorization and renormalization scales.
- 95% CL limits on M_D as a function of the number of extra dimensions are set.

monophoton

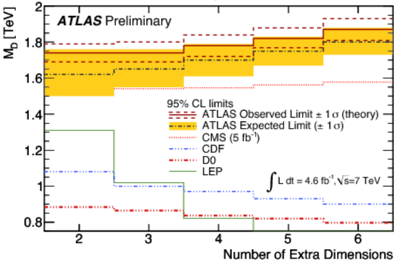

monojet

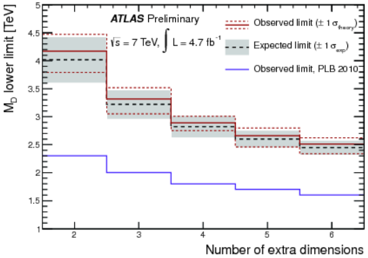

➡ M_D values below 1.74 TeV (n=2) and 1.87 TeV (n=6) are excluded (monophoton).

➡ M_D values below 3.79 TeV (n=2) and 2.34 TeV (n=6) are excluded (monojet).